Radiocarbon, Vol 59, Nr 4, 2017, p 1147–1156 DOI:10.1017/RDC.2017.59
© 2017 by the Arizona Board of Regents on behalf of the University of Arizona. This is an Open Access article, distributed under the terms of the Creative Commons Attribution licence (http://creativecommons.org/licenses/by/4.0/), which permits unrestricted re-use, distribution, and reproduction in any medium, provided the original work is properly cited

RELATIONSHIP BETWEEN SOLAR ACTIVITY AND $\Delta^{14}C$ PEAKS IN AD 775, AD 994, AND 660 BC

Junghun Park[1] • John Southon[2]* • Simon Fahrni[3] • Pearce Paul Creasman[4] • Richard Mewaldt[5]

[1]Korea Institute of Geoscience and Mineral Resources, 124 Gwahang-no, Yuseong-gu, Daejeon 34132, Korea.
[2]Keck/AMS Lab, 3327 Croul Hall, University of California, Irvine, CA 92697, USA.
[3]Laboratory of Ion Beam Physics HPK, Otto-Stern-Weg 5, 8093 Zurich, Switzerland.
[4]Laboratory of Tree-Ring Research, University of Arizona, 1215 E. Lowell Street, Tucson, AZ 85721-0045, USA.
[5]California Institute of Technology, MC: 290-17, Pasadena, CA, 91125 USA.

ABSTRACT. Since the AD 775 and AD 994 $\Delta^{14}C$ peak (henceforth M12) was first measured by Miyake et al. (2012, 2013), several possible production mechanisms for these spike have been suggested, but the work of Mekhaldi et al. (2015) shows that a very soft energy spectrum was involved, implying that a strong solar energetic particle (SEP) event (or series of events) was responsible. Here we present $\Delta^{14}C$ values from AD 721–820 *Sequoiadendron giganteum* annual tree-ring samples from Sequoia National Park in California, USA, together with $\Delta^{14}C$ in German oak from 650–670 BC. The AD 721–820 measurements confirm that a sharp $\Delta^{14}C$ peak exists at AD 775, with a peak height of approximately 15‰ and show that this spike was preceded by several decades of rapidly decreasing $\Delta^{14}C$. A sharp peak is also present at 660 BC, with a peak height of about 10‰, and published data (Reimer et al. 2013) indicate that it too was preceded by a multi-decadal $\Delta^{14}C$ decrease, suggesting that solar activity was very strong just prior to both $\Delta^{14}C$ peaks and may be causally related. During periods of strong solar activity there is increased probability for coronal mass ejection (CME) events that can subject the Earth's atmosphere to high fluencies of solar energetic particles (SEPs). Periods of high solar activity (such as one in October–November 2003) can also often include many large, fast CMEs increasing the probability of geomagnetic storms. In this paper we suggest that the combination of large SEP events and elevated geomagnetic activity can lead to enhanced production of ^{14}C and other cosmogenic isotopes by increasing the area of the atmosphere that is irradiated by high solar energetic particles.

KEYWORDS: 660 BC, AD 775, CME (coronal mass ejection), M12, solar energetic particles (SPE).

INTRODUCTION

The strongest peak of $\Delta^{14}C$, corresponding to the event of AD 775 (called henceforth M12), and another peak in AD 993/4 were measured by Miyake (Miyake et al. 2012, 2013) using ^{14}C in annually resolved Japanese cedar tree-ring sequences, and M12 has been confirmed by several studies (Usoskin et al. 2013; Jull et al. 2014; Güttler et al. 2015; Rakowski et al. 2015; Büntgen et al. 2016) including three that showed peaks with slightly different starting times. Data from high-latitude Siberian and Altai (Jull et al. 2014; Büntgen et al. 2016) record the AD 775 peak but show a $\Delta^{14}C$ rise beginning one year earlier, and $\Delta^{14}C$ data in New Zealand kauri (Güttler et al. 2015) indicate a peak delayed by half a year.

Numerous causes of M12 have been suggested and examined (Thomas et al. 2013), including a supernova (Miyake et al. 2012), a gamma ray burst (GRB) (Hambaryan et al. 2013; Pavlov et al. 2013), and a solar proton event, also known as a solar energetic particle (SEP) event (Melott et al. 2012; Miyake et al. 2012; Thomas et al. 2013; Usoskin et al. 2013; Jull et al. 2014; Mekhaldi et al. 2015.) However, all of these hypotheses have some weak points. If M12 was caused by a supernova, a candidate supernova should exist, but observations spanning several hundred years before AD 775 record no such event. Supernovae emit both high-energy particles and gamma rays, but high-energy particles from supernova have sufficient energy spread that extended arrival times spanning at least 10 yr would be expected (Gehrels 2003; Dee et al. 2017)

*Corresponding author. Email: jsouthon@uci.edu.

Downloaded from https://www.cambridge.org/core. IP address: 50.19.34.255, on 20 Feb 2018 at 19:16:33, subject to the Cambridge Core terms of use, available at https://www.cambridge.org/core/terms. https://doi.org/10.1017/RDC.2017.59

whereas M12 shows a sharp 1–2-yr rise. Gamma rays from supernova and gamma ray bursts have a very short duration time, implying that a short ^{14}C peak could occur, but M12 concentrations of the cosmogenic isotope ^{10}Be measured in Antarctic ice are much too high to have been produced by a GRB (Usoskin et al. 2013). Since no evidence exists for any $\Delta^{14}C$ increase due to an historical SEP event (Jull et al. 2014), any solar phenomenon associated with the M12 peak must have been extremely intense and/or was a much more prolific producer of ^{14}C than those in the instrumental record. However, comparison of M12 ^{10}Be and ^{36}Cl data from polar ice cores (Mekhaldi et al. 2015) show a larger percentage increase over the long term background for ^{36}Cl than ^{10}Be. This result is consistent with production from a flux of relatively soft spectrum of incoming particles (Webber et al. 2007) and hence supports a solar rather than galactic cosmic ray origin for M12.

This study introduces new M12 related $\Delta^{14}C$ data from sequoia tree rings in Sequoia National Park together with German oak $\Delta^{14}C$ values from 650–670 BC and published data (Reimer et al. 2013) that span a $\Delta^{14}C$ peak at 660 BC. Following an analysis and comparisons of our data with the findings of earlier work, the possible causes and processes associated with the M12 peak are discussed.

SAMPLES AND METHODS

Dendrochronological single-year tree-ring samples for AD 721–820 were prepared in the Laboratory of Tree Ring Research (LTRR) at the University of Arizona from sequoia (*Sequoiadendron giganteum*) in Sequoia National Park, California, USA. Sequoia is an evergreen, common in coastal and montane regions of northern California and is among the tallest living trees on Earth. The tree used for this research had rings large enough to ensure that the tested samples contained only material from the precise indicated year, and each ring was subsampled perpendicular to the ring direction to contain an even representation of the year's growth. The samples were treated by acid-base-acid and burned to produce CO_2, which was reduced to graphite and measured at Keck-Carbon Cycle AMS in University of California, Irvine, USA. Additional aliquots of some samples were prepared and measured independently, especially for the decades preceding the M12 spike.

The German oak samples from Oberhaid in Bavaria, Germany, were also prepared as single-year samples at the Institute of Botany, University of Hohenheim, Stuttgart, Germany, and acid-base-acid treated before combustion and subsequent graphitization at Keck-Carbon Cycle AMS.

RESULTS AND DISCUSSION

M12 Peak Analysis

The M12 $\Delta^{14}C$ data for the sequoia are presented and compared with results of Miyake et al. (2012) in Figure 1, while Figure 2 shows six published datasets related to M12 plus results from the present work. Since the Northern Hemisphere (NH) growing season is generally from April to September, the appearance time of M12 in NH datasets is recorded here as AD 775.5 and if a Southern Hemisphere (SH) tree ring showing M12 grew from October AD 774 to April AD 775, the appearance time of M12 is recorded as AD 775.0 (Güttler et al. 2015).

The M12s in five NH datasets appear in AD 775.5, but Siberian larch from 67°31′N (Jull et al. 2014) shows a rise of about 6‰ (< two standard deviations) one year early in AD 774.5, with

Downloaded from https://www.cambridge.org/core. IP address: 50.19.34.255, on 20 Feb 2018 at 19:16:33, subject to the Cambridge Core terms of use, available at https://www.cambridge.org/core/terms. https://doi.org/10.1017/RDC.2017.59

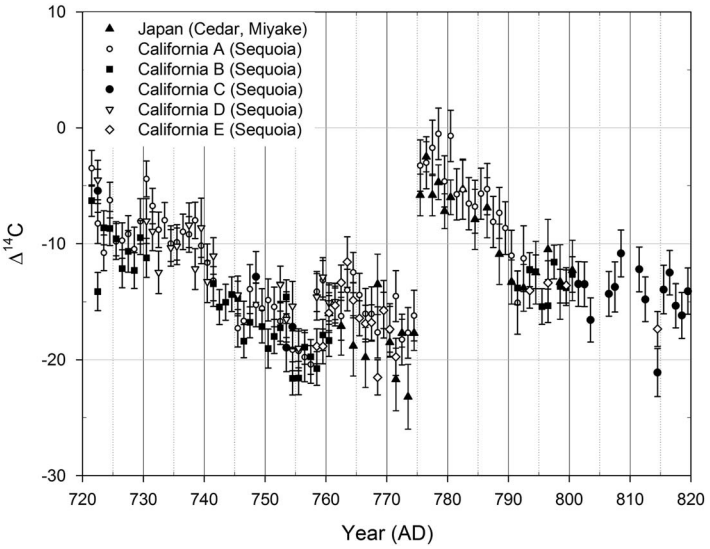

Figure 1 $\Delta^{14}C$ (‰) between AD 721 and 820 in tree rings from sequoia in Sequoia National Park, California, USA, compared to $\Delta^{14}C$ in Japanese cedar (Miyake et al. 2012). The California data include numerous duplicates prepared from the same rings: the A–E designations indicate the time order of treatment and measurement for different batches.

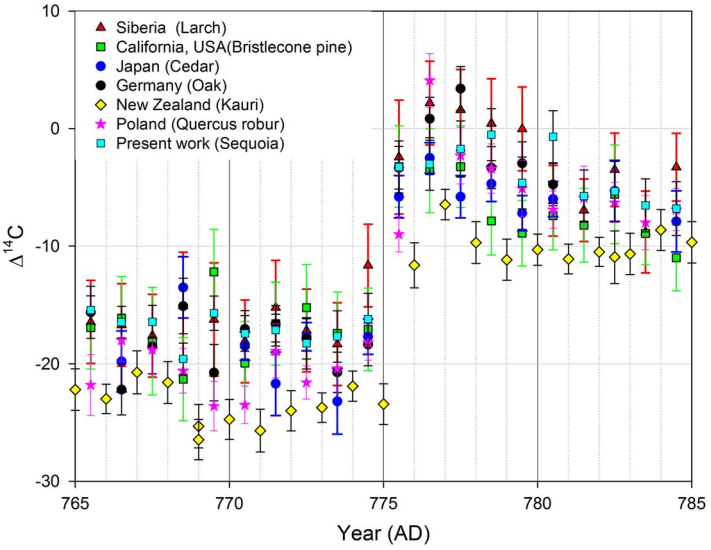

Figure 2 $\Delta^{14}C$ in Siberia (Larch, Jull et al. 2014), California, USA (bristlecone pine, Jull et al. 2014), Japan (cedar, Miyake et al. 2012), Germany (oak, Usoskin et al. 2013), New Zealand (kauri, Güttler et al. 2015), Poland (Quercus, Rakowski et al. 2015) plus average values for California sequoia from this study.

additional increase of 9‰ in AD 775.5 and 2‰ in AD 776.5. The kauri dataset from New Zealand shows M12 appearing 6 months later than in the NH (Güttler et al. 2015), consistent with differences in the NH and SH growing seasons.

Downloaded from https://www.cambridge.org/core. IP address: 50.19.34.255, on 20 Feb 2018 at 19:16:33, subject to the Cambridge Core terms of use, available at https://www.cambridge.org/core/terms. https://doi.org/10.1017/RDC.2017.59

Table 1 Baseline and intensity M12 $\Delta^{14}C$ values plus heights (= intensity-baseline) for datasets shown in Figure 2 (see text for details).

Location	Latitude	Baseline value (‰)	Intensity value (‰)	M12 height (‰)
Japan	30°N	–20.3 ± 1.1	–5.2 ± 0.7	15.0 ± 1.3
Siberia	68°N	–17.2 ± 1.8	–0.4 ± 1.6	16.8 ± 2.4
Germany*	50°N	–18.1 ± 0.8	–1.4 ± 0.8	16.7 ± 1.2
Poland	50°N	–21.1 ± 0.9	–2.7 ± 1.0	18.4 ± 1.4
California (bristlecone)	38°N	–17.3 ± 1.8	–6.2 ± 1.4	11.1 ± 2.3
California (sequoia)	36°N	–17.6 ± 0.9	–2.1 ± 1.0	15.5 ± 1.4
New Zealand	36°S	–23.8 ± 0.8	–9.7 ± 0.7	14.1 ± 1.0

*Average of data from two laboratories (Usoskin et al. 2013)

For a more detailed comparison (Table 1) we define baseline and intensity values for M12. The baseline is defined as the 4-yr $\Delta^{14}C$ average for AD 770.5–773.5 in the NH (the AD 774.5 point is not used, due to the possible early $\Delta^{14}C$ rise in AD 774.5 in the Siberian record) and that for AD 771.0–774.0 in SH. The NH intensity value is defined as the 5-yr average for AD 776.5–780.5, (the AD 775.5 point is not used since some records show $\Delta^{14}C$ still rising in AD 775.5) and the average for AD 777.0–781.0 is used for the SH intensity value. The baseline and intensity values in the present work are higher by 2.7 ± 1.4‰ and 3.1 ± 1.2‰ than those of Miyake et al. (2012) respectively, similar to most of the other NH data: whether this represents a real geographic difference or simply an interlaboratory offset is presently unknown. The baseline and intensity values from New Zealand are ~6‰ lower than the European and U.S. data, consistent with measured NH-SH offsets over the last two millennia (Hogg et al. 2013; Reimer et al. 2013). Given the uncertainties for the M12 heights, the magnitude of the M12 spike is essentially identical for six of the seven records, and although the M12 height for the bristlecone pine record is low, it is nevertheless within two standard deviations of the mean of the other six datasets.

The early (774 AD) rise in the Siberian and Altai $\Delta^{14}C$ data is difficult to reconcile with ^{14}C results from the 1960s, when high-yield Soviet atmospheric nuclear tests in Novaya Zemlya (~74°N) in September–November 1961 and again in the latter half of 1962 produced very high burdens of excess ^{14}C in the NH stratosphere (Feely et al. 1966). After each major injection, measurements of atmospheric $^{14}CO_2$ in air samples from NH ground stations (Nydal and Lovseth 1983; Levin et al. 1985) showed a sharp rise beginning in the early spring of the following year and continuing through the entire NH growing season. By 1963 when the largest ^{14}C increases were observed, a large network of sampling stations extending from 78°N to 9°N was in place (Nydal and Lovseth 1983) and recorded an essentially synchronous $\Delta^{14}C$ rise for all stations. Since no anomalous early high-latitude tropospheric $^{14}CO_2$ signal in a bomb peak was observed, it seems unlikely that any of the mechanisms put forward to explain the M12 peak from a high latitude like Siberia's could generate an equivalent early ^{14}C spike in biomass. Hence, confirmations are required from measurements at other high-latitude sites.

As Figure 2 shows, the M12 peak is delayed in New Zealand kauri, but the delay is consistent with the differences in timing of the NH and SH growing seasons. Furthermore, whereas the maximum SH tropospheric ^{14}C increase during the bomb spike was just 70% of mid-latitude NH values (Manning et al. 1990), reflecting the fact that close to 100% of the input was generated within the NH, the M12 amplitude in the kauri is ~90% of the mean of the NH stations (Table 1), indicating that significant ^{14}C production occurred in both hemispheres.

Downloaded from https://www.cambridge.org/core. IP address: 50.19.34.255, on 20 Feb 2018 at 19:16:33, subject to the Cambridge Core terms of use, available at https://www.cambridge.org/core/terms. https://doi.org/10.1017/RDC.2017.59

Large-scale stratospheric air transport is dominated by the so-called Brewer-Dobson circulation (Butchart 2014) characterized by injection of tropospheric air into the stratosphere in the tropics and subsequently by movement towards the winter pole and subsidence at high latitudes, driven primarily by seasonally varying large-scale eddy motions that act to reduce the mean zonal velocity of air parcels and thus induce a poleward drift (Holton et al. 1995). Descending air in the winter polar vortex carrying a high burden of stratospheric tracers is released near the tropopause when the vortex breaks up in the spring, and extratropical injection of stratospheric air into the troposphere peaks in mid-to-late summer (Stohl et al. 2003). Hence in both hemispheres, tropospheric $^{14}CO_2$ concentrations in the years following the bomb spike showed seasonal cycles, with $\Delta^{14}C$ increasing through the spring and summer and reaching a maximum near the end of the growing season (Nydal and Lovseth 1983; Levin et al. 1985; Manning et al. 1990).

The M12 radiocarbon (^{14}C) was produced simultaneously in both hemispheres according to globally measured data and the events occurred in both hemispheres are undoubtedly confirmed by ^{10}Be data from Greenland and Antarctic ice cores (Sigl et al. 2015). Based on this situation, we infer that this occurred in the early months of 775 AD, at the end of the northern winter. The timing was early enough (and sufficient production was generated low in the stratosphere) that the NH stations received high-^{14}C air when cross-tropopause exchange occurred in the NH spring and summer of 775 AD, and hence the signal was recorded in NH wood produced in mid-year. However, the event took place in the end of SH summer so that little or no ^{14}C was injected into troposphere in that hemisphere during the 774/775 AD austral growing season, and the signal only appeared in the New Zealand kauri in the 775/776 AD ring, almost a year after the production event.

The 660 BC Peak and Solar Activity

Figure 3 shows $\Delta^{14}C$ data covering the period from 550 to 750 BC including single year European oak results from this study. A sharp peak with a rise time of 3–4 yr and amplitude of

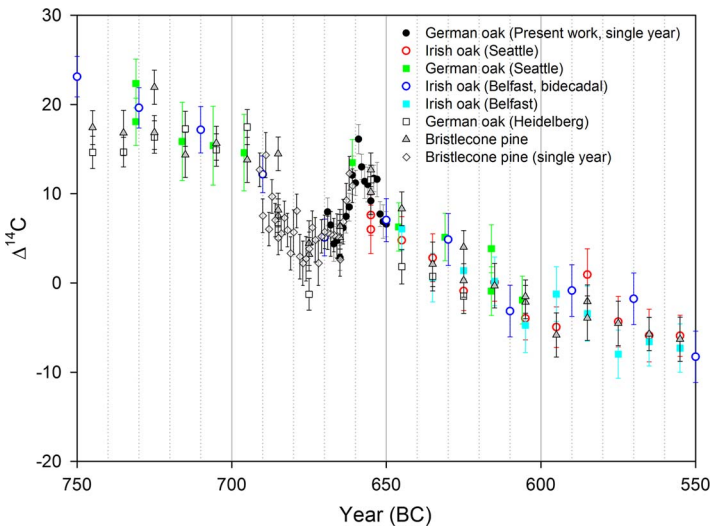

Figure 3 Single-year $\Delta^{14}C$ data in German oak spanning the 660 BC peak (this work) are shown together with single-year and decadal data from IntCal13 (Reimer et al. 2013).

Downloaded from https://www.cambridge.org/core. IP address: 50.19.34.255, on 20 Feb 2018 at 19:16:33, subject to the Cambridge Core terms of use, available at https://www.cambridge.org/core/terms. https://doi.org/10.1017/RDC.2017.59

10‰ is present at 660 BC. Although the rise time of the 660 BC peak is longer than that of M12 and the height of the peak is lower, the peaks in several of the M12 records actually take 2 yr to reach their maximum value (Figure 2), and we suggest that the two peaks were probably produced by similar processes and more measurement of the 660 BC peak are needed for confirmation.

The $\Delta^{14}C$ data in Figure 1 show a decreasing trend (~0.2‰/yr) from 721 to 774 AD and distinct periodic variations of an 11-yr solar cycle [the Schwabe cycle, average variation is a few per mil (‰)] are seen on both sides of the M12 peak (Güttler et al. 2015). This suggests that an interval of several decades prior to M12 showed elevated solar activity, characterized by a strong solar cycle and low ^{14}C production due to enhanced heliomagnetic shielding against galactic cosmic rays. The decadal $\Delta^{14}C$ data from 725 to 675 BC in Figure 3 also show a decreasing trend, suggesting that the 660 BC peak was also preceded by a period of strong solar activity. Any downturn in $\Delta^{14}C$ immediately preceding the single-year AD 994 peak, which Miyake et al. (2013) suggest is also similar to M12, was very small and short-lived at best, but we note that this peak did occur within an interval of generally low $\Delta^{14}C$. Hence although additional research and data are needed, there is some evidence suggesting that these short-lived $\Delta^{14}C$ peaks are correlated with intervals of strong solar activity, and the simplest explanation is that all three have a common cause.

Solar Proton Events and Coronal Mass Ejections

Why could a relationship between strong solar activity and the $\Delta^{14}C$ peaks exist? Mekhaldi et al. (2015) have pointed out that the high $^{36}Cl/^{10}Be$ ratios for the M12 and AD994 peaks in polar ice are consistent with production by relatively low energy particles (tens to hundreds of MeV) and hence point to SEPs rather than galactic cosmic rays (GeV energies) as the source. SEP events occur more frequently during strong solar activity periods (Kurt et al. 2004), and the probability for very intense SEP events increases concurrently. A hypothesized explanation for M12 and similar $\Delta^{14}C$ peaks is that the Earth was irradiated by particles from one or more SEP events involving extremely intense particle fluxes, preferably characterized by unusually harder energy spectra than those of most SEP events. The lower energy SEP component is deflected by Earth's magnetic field and cannot interact with the atmosphere except at the poles, but the high energy tail of the energy spectrum may have contained a sufficiently high fluence of protons to generate the observed burden of cosmogenic isotopes. Recently, superflares from Sun-like stars were observed with a thousand times the energy release of the largest flares on our Sun, although the life stage at which Sun-like stars make superflares and differences between the Sun and Sun-like stars are still under debate (Maehara et al. 2012, 2015).

This is a popular theory (Miyake et al. 2012; Usoskin et al. 2013; Jull et al. 2014; Mekhaldi et al. 2015) but a potential problem is that it requires a SEP fluence at least five times larger than for any event recorded in the era of ground-based or satellite observations (Mekhaldi et al. 2015). Therefore, we consider the fact that large SEP events are often also associated with large geomagnetic storms (Li et al. 2006), which can have the effect of enlarging the area of the atmosphere that is irradiated by solar energetic particles (Leske et al. 2001).

Here we suggest a possible solution to this difficulty, based on the association of SEPs with coronal mass ejection events (CMEs). A CME occurs when magnetic disturbances on the Sun lead to the violent ejection of a large volume of plasma into interplanetary space, in the form of an expanding thick shell that can extend over angular ranges of 120° or more, anchored at the source region on the Sun. Since the velocities of fast CMEs can reach ~2500–3000 km/s, far

Downloaded from https://www.cambridge.org/core. IP address: 50.19.34.255, on 20 Feb 2018 at 19:16:33, subject to the Cambridge Core terms of use, available at https://www.cambridge.org/core/terms. https://doi.org/10.1017/RDC.2017.59

greater than the ~350–750 km/s speed of the solar wind, a shockwave forms in front of the CME and the shocked solar wind plasma and the CME itself both contain embedded magnetic fields that interact and reconnect with the geomagnetic field. Fast CMEs are almost always accompanied by solar flares, but typically most of the associated SEPs are not from the flare itself, but are solar wind and suprathermal ions (mainly protons) and electrons accelerated to tens to thousands of MeV by the expanding CME shockwave (Gosling 1993; Reames 1999). Since protons at these energies outrun the shock, SEP arrival at the Earth typically begins 1–2 days prior to the interaction of the shockwave and the CME with the geomagnetic field. In the largest events a reservoir forms in the inner heliosphere (Reames et al. 1997) and elevated particle fluxes may persist for a week or more.

The fastest CMEs can reach Earth in a day or less and if the flare site is located near the central meridian the geomagnetic storm can often commence while SEP intensities are near their maximum. Examples include the August 4, 1972, and July 14, 2000, events, among the largest of the space era. In addition, Gopalswamy et al. (2004) and Li et al. (2012) have shown that many CMEs involving especially high fluences of SEPs are twin events where a second CME erupts within 24 hours of the first. The ^{14}C production from the two events would add nearly linearly (Melott et al. 2012). Additionally the passage of the initial shockwave leaves a region in its wake that for several hours contains high densities of suprathermal particles and elevated levels of solar wind turbulence. If a second shock arrives before the suprathermal decay, it had been suggested that particles are apparently accelerated with greater efficiency, producing a hard SEP flux that will generate unusually large numbers of secondary neutrons and correspondingly high levels of ^{14}C. Gopalswamy et al. (2004) find that the second of these two events is typically more intense by a median value of ~7. Furthermore, if the first CME and/or the shocked plasma in front of it contain strong embedded southward-pointing magnetic fields, these southward fields reconnect with the north-directed fields on the front side of the magnetosphere, releasing a large amount of energy. The resulting magnetic storm acts to reduce the geomagnetic field, so that when SEPs accelerated by the second shock reach the neighborhood of the Earth, they may encounter greatly reduced geomagnetic cutoffs and hence can reach an abnormally large fraction of the atmosphere (Leske et al. 2001; Kress et al. 2010).

To our knowledge, this hypothesis of a synergy between unusually intense and high energy SEPs and reduced geomagnetic shielding has not been considered in the derivation of particle fluences required to explain the M12 peak, but elements of it are certainly consistent with CME and SEP observations. Twin CMEs occur relatively frequently (Li et al. 2012; Ding et al. 2013) and multiple large events within a few days (often from the same active region) are common. Gopalswamy et al. (2004) reported that most of the large SEP events originating from CME-driven shock acceleration in 1997 to early 2002 were preceded by an earlier CME-driven shock event originating from the same solar active region within 24 hours earlier. For example, 80 CMEs, numerous intense flares, and five large SEP events occurred over a three-week period in October–November 2003, the four largest from a single, very active region on the Sun (Gopalswamy et al. 2005; Mewaldt et al. 2005). Furthermore, over several periods of some hours within this sequence, the geomagnetic cutoff latitude for 19–27 MeV protons was reduced from 65° to 50–55° (Kress et al. 2010), corresponding approximately to doubling of the fraction of the atmosphere exposed to those particles. The Carrington Event of 1859 involved major magnetic storms on August 28–29 and September 2–3, with auroras visible at geomagnetic latitudes as low as 25° and 18°, respectively (Green and Boardsen 2006), suggesting that two closely spaced CMEs interacted strongly with the geomagnetic field. As noted by Jull et al. (2014), there is no evidence for this event in the annual ^{14}C record, which at first sight appears to

Downloaded from https://www.cambridge.org/core. IP address: 50.19.34.255, on 20 Feb 2018 at 19:16:33, subject to the Cambridge Core terms of use, available at https://www.cambridge.org/core/terms. https://doi.org/10.1017/RDC.2017.59

challenge the hypothesis outlined above, but we have no information on the intensity, spectrum, and duration of the SEP event and the conditions for efficient particle acceleration leading to a very hard energy spectrum may not have been met (Li et al. 2006).

CONCLUSION

New $\Delta^{14}C$ data from AD 721–820 from sequoia tree rings of California, USA, are presented and compared with the result of Miyake et al. (2012). The calculated M12 height of 15.5 ± 1.4‰ and the appearance time of AD 775 for M12 in our record are same to those of Miyake et al. (2012). Based on the amplitude and timing of the corresponding peaks in other NH records and in New Zealand kauri, ^{14}C spike production was a global event and probably occurred in the late northern winter (January or February) of AD 775. $\Delta^{14}C$ data from 550–750 BC from both the present study and Reimer et al. (2013) show that a sharp 10‰ peak with a rise time of 3–4 yr is present at 660 BC. Although the 660 BC rise time is longer than that of M12 and the height is lower, both peaks appear during periods of strong solar activity, and the simplest explanation for the 660 BC and AD 994 spikes and M12 is that all three have a common cause.

The high $^{36}Cl/^{10}Be$ ratios for the M12 and AD 994 peaks in polar ice (Mekhaldi et al. 2015) support a relatively soft energy spectrum, consistent with production by accelerated solar particles rather than galactic cosmic rays, but the SEP fluxes required are far larger than any of those in the instrumental SEP record. However, if a southward-pointing magnetic field associated with an intense CME event reconnects with the geomagnetic field, an unusually large fraction of the atmosphere may be exposed to particles accelerated efficiently by the shock wave associated with a closely following second CME (Li et al. 2012). The synergistic effects of reduced geomagnetic cutoffs and hard SEP spectra could lead to unusually effective production of ^{14}C and other cosmogenic isotopes, and hence the calculated values for the required particle fluences may be too large. In addition, the largest events often occur during a period of elevated solar activity when elevated SEP intensities and geomagnetic storms can continue for weeks. Evidence for sharp reductions in geomagnetic cutoff values during CMEs and for multi-CME sequences leading to unusually efficient particle acceleration does exist, but determining whether this mechanism can provide a quantitative explanation for the observed ^{14}C spikes will require detailed calculations in future studies.

ACKNOWLEDGMENTS

This study was supported by a research project funded by the Ministry of Science, ICT and Future Planning of Korea. We are grateful for helpful and constructive comments from F Miyake and F Mekhaldi. The work at Caltech was supported by NASA under NNX13A66G, and subcontract 00008864 of NNX15AG09G, and by the NSF under grant AGS-1622487.

SUPPLEMENTARY MATERIAL

To view supplementary material for this article, please visit https://doi.org/10.1017/RDC.2017.59.

REFERENCES

Büntgen U, Myglan VS, Ljungqvist FC, McCormick M, Di Cosmo N, Sigl M, Jungclaus J, Wagner S, Krusic PJ, Esper J, Kaplan JO, de Vaan MAC, Luterbacher J, Wacker L, Tegel W, Kirdyanovet AV. 2016. Cooling and societal change during the late antique little ice age from 536 to around 660 AD. *Nature Geoscience* 9:231–6. DOI: 10.1038/NGEO02652.

Butchart N. 2014. The Brewer-Dobson circulation. *Reviews of Geophysics* 52:157–84.

Downloaded from https://www.cambridge.org/core. IP address: 50.19.34.255, on 20 Feb 2018 at 19:16:33, subject to the Cambridge Core terms of use, available at https://www.cambridge.org/core/terms. https://doi.org/10.1017/RDC.2017.59

Dee M, Pope B, Miles D, Manning S, Miyake F. 2017. Supernovae and single-year anomalies in the atmospheric radiocarbon record. *Radiocarbon* 59(2):293–302. DOI: 10.1017/RDC.2016.50.

Ding L, Jiang Y, Zhao L, Li G. 2013. The "twin-CME" scenario and large solar energetic particle events in solar cycle 23. *The Astrophysical Journal* 763:30.

Feely HW, Seitz H, Lagomarsino RJ, Biscaye PE. 1966. Transport and fallout of stratospheric radioactive debris. *Tellus* 18(2):316–28.

Gehrels N, Laird CM, Jackman CH, Cannizzo JK, Mattson BJ, Chen W. 2003. Ozone depletion from nearby supernovae. *The Astrophysical Journal* 585:1169–76.

Gopalswamy N, Yashiro S, Krucker S, Stenborg G, Howard RA. 2004. Intensity variation of large solar energetic particle events associated with coronal mass ejections. *Journal of Geophysical Research* 109:A12105.

Gopalswamy N, Yashiro S, Michalek G, Xie H, Lepping RP, Howard RA. 2005. Solar source of the largest geomagnetic storm of cycle 23. *Geophysical Research Letters* 32:L12S09. DOI: 10.1029/2004GL021639.

Gosling JT. 1993. The solar flare myth. *Journal of Geophysical Research* 98:18937–49.

Green JL, Boardsen S. 2006. Duration and extent of the great auroral storm of 1859. *Advances in Space Research* 38:130–5.

Güttler D, Adolphi F, Beer J, Bleicher N, Boswijk G, Christl M, Hogg A, Palmer J, Vockenhuber C, Wacker L, Wunder J. 2015. Rapid increase in cosmogenic ^{14}C in AD 775 measured in New Zealand kauri trees indicates short-lived increase in ^{14}C production spanning both hemispheres. *Earth and Planetary Science Letters* 411:290–7.

Hambaryan VV, Neuhäuser R. 2013. Galactic short gamma-ray burst as cause for the ^{14}C peak in AD 774/5. *Monthly Notices of the Royal Astronomical Society* 430:32–6.

Hogg AG, Hua Q, Blackwell PG, Mu N, Buck CE, Guilderson TP, Heaton TJ, Palmer JG, Reimer PJ, Reimer RW, Turney CSM, Zimmerman SRH. 2013. SHCal13 Southern Hemisphere calibration, 0–50,000 years cal BP. *Radiocarbon* 55(4): 1889–903.

Holton JR, Haynes PH, McIntyre ME, Douglass AR, Rood RB, Pfister L. 1995. Stratosphere-troposphere exhange. *Reviews of Gephysics* 33(4): 403–39.

Jull AJT, Panyushkina IP, Lange TE, Kukarskih VV, Myglan VS, Clark KJ, Salzer MW, Burr GS, Leavitt SW. 2014. Excursions in the ^{14}C record at AD 774–775 in tree rings from Russia and America. *Geophysical Research Letters* 41. DOI: 10.1002/2014GL059874.

Kress BT, Mertens CJ, Wiltberger M. 2010. Solar energetic particle cutoff variations during the 29–31 October 2003 geomagnetic storm. *Space Weather* 8:S05001. DOI: 10.1029/2009SW000488.

Kurt V, Belov QA, Mavromichalaki H, Gerontidou M. 2004. Statistical analysis of solar proton events. *Annales Geophysicae* 22:2255–71.

Leske RA, Mewaldt RA, Stone EC, Rosenvinge TT. 2001. Observations of geomagnetic cutoff variations during solar energetic particle events and implications for the radiation environment at the space station. *Journal of Geophysical Research* 106:30011–22.

Levin I, Kromer B, Schoch-Fischer H, Bruns M, Münnich M, Berdau D, Vogel JC, Münnich KO. 1985. 25 years of tropospheric ^{14}C observations in Central Europe. *Radiocarbon* 27(1):1–19.

Li G, Moore R, Mewaldt RA, Zhao L, Labrador AW. 2012. A twin-CME scenario for ground level enhancement events. *Space Science Reviews* 171: 141–60.

Li X, Temerin M, Tsurutani BT, Alex S. 2006. Modeling 1–2 September 1859 super magnetic storm. *Advances in Space Research* 38:273–9.

Maehara H, Shibayama T, Notsu S, Notsu Y, Nagao T, Kusaba S, Honda S, Nogami D, Shibata K. 2012. Superflares on solar-type stars. *Nature* 485:478–81.

Maehara H, Shibayama T, Notsu Y, Notsu S, Honda S, Nogami D, Shibata K. 2015. Statistical properties of superflares on solar-type stars based on 1-min cadence data. *Earth, Planets and Space* 67:59.

Manning MR, Lowe DC, Melhuish WH, Sparks RJ, Wallace G, Brenninkmeijer CAM, McGill RC. 1990. The use of radiocarbon measurements in atmospheric studies. *Radiocarbon* 32(1):37–58.

Mekhaldi F, Muscheler R, Adolphi F, Aldahan A, Beer J, McConnell JR, Possnert G, Sigl M, Svensson A, Synal H-A, Welten KC, Woodruff TE. 2015. Multiradionuclide evidence for the solar origin of the cosmic-ray events of AD 774/5 and 993/4. *Nature Communications* 6:8611. DOI: 10.1038/ncomms9611.

Melott AL, Thomas BC. 2012. Causes of an AD 774–775 ^{14}C increase. *Nature* 491:E1–2.

Mewaldt RA, Cohen CMS, Labrador AW, Leske RA, Mason GM, Desai MI, Looper MD, Mazur JE, Selesnick RS, Haggerty DK. 2005. Proton, helium, and electron spectra during the large solar particle events of October–November 2003. *Journal of Geophysical Research* 110:A09S18. DOI: 10.1029/2005JA011038.

Miyake F, Nagaya K, Masuda K, Nakamura T. 2012. A signature of cosmic-ray increase in AD 774–775 from tree rings in Japan. *Nature* 486:240–2.

Miyake F, Masuda K, Nakamura T. 2013. Another rapid event in the carbon-14 content of tree rings. *Nature Communications* 4:1748. DOI: 10.1038/ncomms2783.

Nydal R, Lövseth K. 1983. Tracing bomb ^{14}C in the Atmosphere 1962–1980. *Journal of Geophysical Research* 88:3621–42.

Pavlov AK, Blinov AV, Konstantinov AN, Ostryakov VM, Vasilyev GI, Vdovina MA, Volkovet PA. 2013. AD 775 pulse of cosmogenic radionuclides

Downloaded from https://www.cambridge.org/core. IP address: 50.19.34.255, on 20 Feb 2018 at 19:16:33, subject to the Cambridge Core terms of use, available at https://www.cambridge.org/core/terms. https://doi.org/10.1017/RDC.2017.59

production as imprint of a galactic gamma-ray burst. *MNRAS* 435:2878–84.

Rakowski AZ, Krapiec M, Huels M, Pawlyta J, Dreves A, Meadows J. 2015. Increase of radiocarbon concentration in tree rings from Kujawy (SE Poland) around AD 774–775. *Nuclear Instruments and Methods in Physics Research B* 361:564–8.

Reames DV. 1999. Particle acceleration at the sun and in the heliosphere. *Space Science Reviews* 90: 413–91.

Reames DV, Kahler SW, Ng CK. 1997. Spatial and temporal invariance in the spectra of energetic particles in gradual solar events. *The Astrophysical Journal* 491:414–20.

Reimer PJ, Bard E, Bayliss A, Beck JW, Blackwell PG, Bronk Ramsey C, Buck CE, Cheng H, Edwards RL, Friedrich M, Grootes PM, Guilderson TP, Haflidason H, Hajdas I, Hatte C, Heaton TJ, Hoffman DL, Hogg AG, Hughen KA, Kaiser KF, Kromer B, Manning SW, Niu M, Reimer RW, Richards DA, Scott EM, Southon JR, Staff RA, Turney CSM, van der Plicht J. 2013. IntCal13 and Marine13 radiocarbon age calibration curves 0–50,000 years cal BP. *Radiocarbon* 55(4):1869–87.

Sigl M, Winstrup M, McConnell JR, et al. 2015. Timing and climate forcing of volcanic eruptions for the past 2,500 years. *Nature* 523:543–9.

Stohl A, Bonasoni P, Cristofanelli P, et al. 2003. Stratosphere-troposphere exchange: A review, and what we have learned from STACCATO. *Journal of Geophysical Research* 108(D12). DOI: 10.1029/2002JD002490.

Thomas BC, Melott AL, Arkenberg KR, Snyder BR II. 2013. Terrestrial effects of possible astrophysical sources of an AD 774–775 increase in ^{14}C production. *Geophysical Research Letters* 40:1237–40.

Usoskin IG, Kromer B, Ludlow F, Beer J, Friedrich M, Kovaltsov GA, Solanki SK, Wacker L. 2013. The AD775 cosmic event revisited: the Sun is to blame. *Astronomy & Astrophysics* 552:L3. DOI: 10.1051/0004-6361/201321080.

Webber WR, Higbie PR, McCracken KG. 2007. Production of the cosmogenic isotopes ^{3}H, ^{7}Be, ^{10}Be, and ^{36}Cl in the Earth's atmosphere by solar and galactic cosmic rays. *Journal of Geophysical Research* 112:A10106. DOI: 10.1029/2007JA012499.

Downloaded from https://www.cambridge.org/core. IP address: 50.19.34.255, on 20 Feb 2018 at 19:16:33, subject to the Cambridge Core terms of use, available at https://www.cambridge.org/core/terms. https://doi.org/10.1017/RDC.2017.59